研 究 速 報

UDC 539.388.1
669.384-172

FATIGUE CRACKS UNDER PLANE STRESS IN ELECTRO-DEPOSITED COPPER SINGLE CRYSTALS–PART I

平面応力下における電着銅単結晶の疲れき裂 (1)

By Masahisa MATSUNAGA* and Yoshiaki HAGIUDA*
松 永 正 久・萩 生 田 善 明

1. Introduction

In the previous reports, the authors observed uniformly distributed cracks generated on surfaces of electrodeposited copper on ABS plastics[1)2)]. These cracks were originated by the plane stress in copper, because of difference in Youngs' modulus between both materials. In this report, the same method is applied to copper single crystal films in order to examine fine structure of the uniformly distributed cracks, its dependence on crystal orientation and process of occurence of the cracks

2. Experimental methods

(1) Specimens

Copper single crystals were Electrodeposited by the method developed by Sard and Weil[3)]. In order to fix the single crystals (10 mm square) on plastics of the shape of Fig. 1, a procedure of Fig. 2 was adopted.

A single crystal of KCl, 10 mm square and 2 mm thick, was made by cleavage and copper films were epitaxially evaporated on the crystal heated at 340°C. The thickness of the copper films was about 0.2 μm and the surface had {001}. After cooling slowly, the film on KCl was pasted

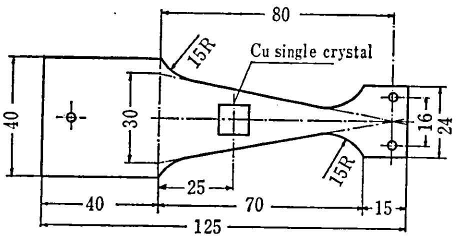

Fig. 1 Shape of a speciment

* Dept. of Mechanical Engineering and Naval Architecture, Inst. of Industrial Science, Univ. of Tokyo.

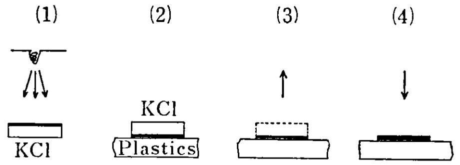

Fig. 2 Preparing method of a electrodeposited copper single crystal on plastics.
(1) evaporation (2) adherence
(3) dissolve KCl in water
(4) electrodeposition

on the plastics specimen. KCl was dissolved off in water. The copper single crystal was deposited in 1 N copper sulfate bath at the current density of 2 mA/cm^2. After deposition, the surface was electropolished in 70 per cent phosphoric acid bath at the temperature of 2°C in order to remove the surface asperities.

(2) Fatigue test

Fatigue tests were performed by a repeated bending machine of 210 cpm. The strain amplitude ε was $15{\sim}17\times10^{-4}$ and number of repeats N was $1{\sim}3\times10^5$. Directions of stress were

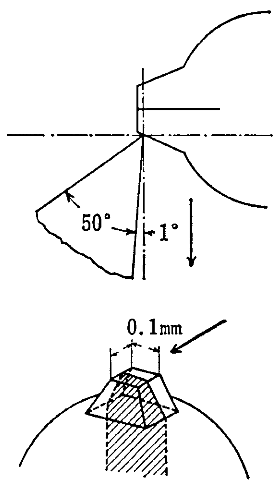

Fig. 3 Cutting system by a microtome. Arrows indicates cutting direction. The hatched part is a copper film.

〔100〕, 〔110〕 and 〔210〕 and the crystal orientation was decided when the evaporated film was pasted on the specimen.

(3) **Observation methods for fine structure**

Optical and Electron microscopes were used for observing the fatigued surfaces. In order to observe extusions and intrusions, thin films of 500∼1000 Å thick were cut by a microtome as shown in Fig. 3.

3. Experimental results and discussions

(1) **Generation of the uniformly distributed cracks and their dependency on crystal orientations**

Fig. 4 indicates the uniformly distributed cracks generated on a fatigued specimen when the axis of stress was 〔100〕. In the case of polycrystals, the uniformly distributed cracks were generated along the direction of the maximum shearing stress[2]. However, in the case of the single crystals, the direction of the cracks were fully dependent on the crystal orientation. Cracks always lie along the direction of 〔110〕 and the direction did not depend on the axis of the stress.

Since the free surface of the single crystals was {100}, the surface had four intersections with {111} surfaces. The direction of the intersections

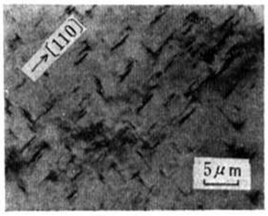

Fig. 4 Typical distributed cracks on a copper single crystal.

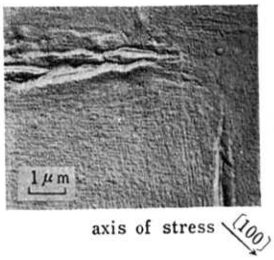

Fig. 5 Distributed cracks. along double slip lines.

was naturally 〔110〕. Generally speaking, the slip plane of FCC metals are {111}, and two slip systems are always working in all tensile directions. Since Schmidt factors for the working slip systems are dependent on the tensile directions, the generation of slip bands has various characteristics. Fig. 6 indicates the maximum Schmidt factor values and differences between the maximum and the following values to the maximum. When the tensile direction coincided

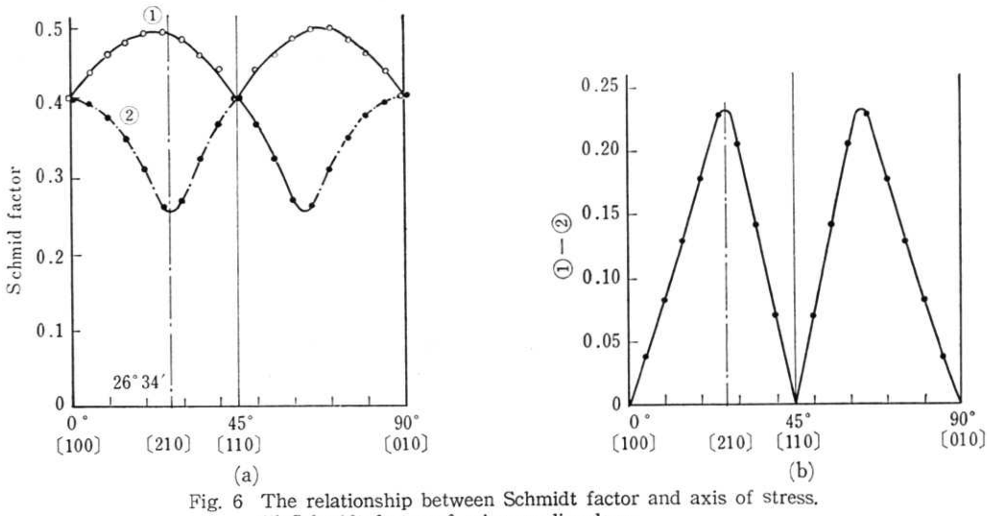

Fig. 6 The relationship between Schmidt factor and axis of stress.
(1) Schmidt factor of primary slip plane
(2) Schmidt factor of secondary slip plane

with 〔100〕, the difference was zero and the cracks became symmetrical with 〔100〕. It corresponded to Figs. 4 and 5 and the symmetrical double slips like a grating appeared as shown in Fig. 5 by electronmicroscopy. Extrusions and intrusions could be observed in the micrograph, and cracks grew from the intrusions in the case of the plane stress.

When the tensile direction was changed to 26°～27°, that is, coincided with 〔210〕, the Schmidt factor became maximum of all directions and the difference also became largest. In other words, the slip bands corresponded to the slip system with the maximum Schmidt factor. Fig. 7a indicates the cracks of this type, and the cracks were originated along one direction. Fig. 7b indicates the electronmicrograph. Although the slip bands near the cracks were also along the direction, the graph contains some cross slips.

Fig. 8 indicates the electron micrograph of the cracks for the tensile direction of 〔110〕. The values of Schmidt factor was symmetrical as in the case of 〔100〕, but the slip direction existed only in two directions, that is, parallel or perpendicular to the tensile direction. The cracks, therefore, were different from that of 〔100〕. However, since the cleavage surface did not exist, slip bands were not arrayed parallel.

(Manuscript received April 16, 1972)

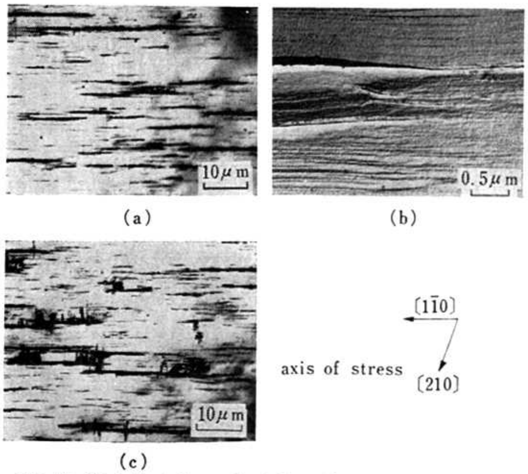

Fig. 7 Distributed cracks lying along one direction.
(a) optical micrograph
(b) electron micrograph
(c) optical micrograph containing cross slips

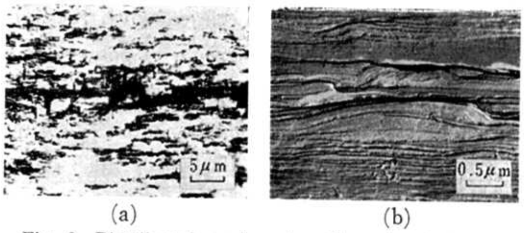

Fig. 8 Distributed cracks when the axis of stress is 〔110〕.

References

1) M. Matsunaga and Y. Hagiuda, Metal Finishing, 69, 4 (1971) 36.
2) M. Matsunaga and Y. Hagiuda, Preprint of 8th Congress of INTERFINISH, Basel, B26, 1972.
3) R. Sard and R. Weil, Electrochimica Acta 15(1970) 1977.